Room-temperature magnetic phases of Fe on fcc Co(001) and Ni(001)

W. L. O'Brien
Synchrotron Radiation Center, University of Wisconsin-Madison, 3731 Schneider Drive, Stoughton, Wisconsin 53589

B. P. Tonner
Synchrotron Radiation Center, University of Wisconsin-Madison, 3731 Schneider Drive, Stoughton, Wisconsin 53589
and Department of Physics, University of Wisconsin–Milwaukee, 1900 East Kenwood Boulevard, Milwaukee, Wisconsin 53211
(Received 20 March 1995)

A sequence of three distinct magnetic phases of Fe are found for growth on both fcc Co(001) and Ni(001) using x-ray magnetic circular dichroism. For Fe coverages below 5 ML the films are ferromagnetic, with the magnetic moments aligned perpendicular to the surface for growth on Ni and parallel to the surface for growth on Co. Between 5 and 11 ML the Fe films are nonmagnetic at room temperature, but include a ferromagnetic live monolayer at the Fe/Co and Fe/Ni interface. The moment of the magnetically live monolayer is aligned perpendicular to the surface for growth on Ni and parallel to the surface for growth on Co. Above 11 ML the Fe films are once again ferromagnetic. An identical sequence of magnetic phase transitions is known to occur for Fe growth on Cu(001). Based on this comparison and on the nearly identical lateral lattice constants of fcc Co, Ni, and Cu, we conclude that Fe growth on fcc Co(001) and Ni(001) follows the same sequence of crystalline phase transitions as Fe growth on Cu(001). Supporting this conclusion are the identical sequence of surface reconstructions observed by low-energy electron diffraction for Fe growth on Co(001) and Cu(001). For Fe/Ni(001) these surface structural changes are not observed, suggesting that details in the growth mode of Fe on Ni are different for Fe on Co and Cu.

I. INTRODUCTION

The study of ultrathin magnetic films on single-crystal substrates has contributed greatly towards our understanding of surface and interface magnetism. An important characteristic of ultrathin films is that the first few monolayers quite often grow in metastable structures that can be different from the bulk phases of the overlayer material. By properly choosing the substrate, film thickness, and growth conditions, different crystalline phases of a magnetic material can be formed. Even small changes in the epitaxial film structure can result in significant modifications to its magnetic properties.[1–12]

Perhaps the most studied magnetic thin film system is Fe/Cu(001).[1–8] These films exhibit a variety of different magnetic properties and crystalline structures depending on growth technique, film thickness, and temperature. Three phases of Fe, identified by their different magnetic properties, are found in films grown at room temperature using physical vapor deposition. Fe films less than 5 monolayers (ML) thick are ferromagnetically ordered, with an easy axis of magnetization perpendicular to the surface.[1,2] Films between 5 and 11 monolayers thick are antiferromagnetic with a Néel temperature below room temperature. The outer two surface layers of this antiferromagnetic phase are ferromagnetically aligned with the moment oriented perpendicular to the surface.[1,2] Films thicker than 11 ML are ferromagnetic with an in-plane moment.[1,2]

These three regions of different magnetic behavior correspond to three distinct surface structures, which can be identified by their low-energy electron diffraction (LEED) patterns.[3] The ferromagnetic phase present at coverages below 5 ML has an $(n\times1)$ LEED pattern, where $n=4$ or 5.[1–3] The antiferromagnetic phase has been reported by various groups to have either a $(1\times1)^2$ or (2×1) (Refs. 1, 3) LEED pattern. For coverages above 11 ML a (3×1) LEED pattern is observed.[1–3] The crystalline structure of these three phases has been investigated by a number of techniques, including x-ray photoelectron diffraction,[10] scanning tunneling microscopy (STM),[8] and extended x-ray absorption fine structure (EXAFS).[4] EXAFS and STM both find evidence of a fcc-to-bcc phase transition as the film thickness increases beyond 10 ML. This identifies the antiferromagnetic Fe phase present between 5 and 11 ML as fcc Fe and the ferromagnetic phase present at coverages above 11 ML as bcc Fe. The low-coverage (<5 ML) ferromagnetic phase has been identified as a face-centered-tetragonal structure by EXAFS,[4] although possible effects of intermixing of substrate atoms cannot be ruled out in this coverage range.[10]

An important open question is whether the metastable fct and fcc structures of Fe can be observed on other substrates, or if they are only present in the Fe/Cu(001) system. It is worthwhile to search for alternative substrates that support the metastable structures of Fe, since the epitaxy of Fe on Cu(100) is not ideal, and it would be valuable to be able to alter the epitaxial lattice constants and growth modes. We have chosen to investigate both fcc Ni(100) and metastable fcc Co(100) as substrates for Fe epitaxy, where the substrates are in the form of films grown on Cu(100). Recently, it has been shown that both Co and Ni grow epitaxially on Cu(001) at room temperature. For Co/Cu(001) the growth mode is nearly perfectly layer by layer, resulting in metastable fcc Co films with the same surface unit cell as Cu(001) (Refs. 9, 10) for films below the critical layer thickness for dislocation formation. Ni on Cu(001) also grows in the fcc structure[12] owing to the close lattice match between Ni and Cu. Because

0163-1829/95/52(21)/15332(9)/$06.00

of the nearly identical surface unit cell of Cu(001), metastable fcc Co(001), and Ni(001), we expect that there is a strong likelihood that the Fe/Co(001) and Fe/Ni(001) structures are very similar to those of Fe/Cu(100), although the details of the growth mode may be different owing to the difference in interface energies and surface free energies of the systems. Considering thermodynamic arguments alone, Fe is more likely to grow layer by layer on Ni or Co than on Cu since both Ni and Co have higher surface free energies than Cu.

Although all three substrates have similar lattice parameters, the fcc Co(001) and Ni(001) substrates are ferromagnetic, and so it is of interest to determine how these substrates alter the magnetism of fct and fcc metastable Fe thin films. The fcc Co/Cu(001) films are ferromagnetically ordered with an in-plane, $\langle 110 \rangle$, easy axis of magnetization.[13] At room temperature ferromagnetic ordering is present for films thicker than 2 ML.[13] The ferromagnetic ordering of Ni/Cu(001) films has an unusual dependence on film thickness.[14–16] For films between 5 and 9 ML thick, at room temperature, ferromagnetic ordering is observed with an easy axis of magnetization in the surface plane. For films thicker than 9 ML the easy axis of magnetization is perpendicular to the film surface. This unusual behavior persists for film coverages up to ~40 ML.

Much of the detailed information on the magnetic phase diagram of Fe on Cu(100) has come from surface magneto-optic Kerr effect (SMOKE) measurements.[1,2,10] In the optical wavelength region, the Kerr effect is not selective for particular elemental species, so that in complex multilayer magnetic samples, the SMOKE averages over the magnetization of all material within a few hundred angstroms of the surface. This limitation has prevented a detailed study of the magnetic phase diagram of ferromagnetic ultrathin films grown on magnetically active substrates. X-ray magnetic circular dichroism (XMCD) is a relatively newer technique which has been shown to be useful for the study of magnetic thin films.[7,13,14,17–19] The XMCD signal in transition metals is tied to core levels that are widely separated in energy from element to element, so that element-specific magnetometry is now possible.[19] We use this capability to study the magnetic phase diagrams of ferromagnetic films grown on magnetic substrates.

The XMCD signal $\sigma_M = \sigma_+ - \sigma_-$ is the difference between the x-ray absorption spectra with the photon spin vector parallel (σ_+) and antiparallel (σ_-) to the sample magnetization. The absolute value of the XMCD intensity at the L_3 edge, $|\sigma_M(L_3)|$, can be used to monitor the degree of long-range magnetic ordering, since it is proportional to the net magnetization. By normalizing $|\sigma_M(L_3)|$ to the total absorption cross section at L_3, $\sigma_0(L_3) = 1/2[\sigma_+(L_3) + \sigma_-(L_3)]$, we obtain an important intensive quantity: the magnetization or degree of ferromagnetic ordering on a per atom basis. For convenience we introduce the symbol Σ to represent the normalized dichroism intensity, $\Sigma = |\sigma_M(L_3)/\sigma_0(L_3)|$. Through the vector character of the dichroism signal, we measure the net vector magnetization per atom in the sample: $\Sigma \propto \langle M \rangle$.

In this paper we report on the magnetism and structure of ultrathin Fe films grown on the ferromagnetic substrates fcc Co(001) and fcc Ni(001). A comparison is made to measurements made also on Fe/Cu(100). The fcc Co(001) substrate was grown as a metastable fcc ultrathin layer on Cu(001) to thicknesses of about 10 ML, which is below the critical layer thickness for relaxation of the strained epitaxial Co layer.[9] The fcc Ni(001) substrate used was in the form of a 15 ML film grown on Cu(001). These film thickness were chosen to reduce the possibility of Cu diffusion to the surface. Also, while both these substrates are ferromagnetic, the direction of their net magnetization is very much different, being in the surface plane for Co and perpendicular to the surface plane for Ni. We find that the surface structures and sequence of magnetic phases of Fe on Co(001), Ni(001), and Cu(001) are nearly identical. We also show that the ferromagnetism of the Ni and Co substrates influences the magnetic ordering of the metastable Fe films.

II. EXPERIMENTAL METHODS

The experiments were performed on the 10 M toroidal grating monochromator beam line located at the Synchrotron Radiation Center. The beam line is equipped with a water-cooled copper aperture which allows the selection of either linear, left-handed, or right-handed circularly polarized photons. The degree of circular polarization is 85%, as determined by calculation.[20] The experimental apparatus includes a growth chamber, for sample cleaning, film deposition and LEED, and a measurement chamber, for XMCD. The measurement chamber was located between the poles of an electromagnet with a maximum field strength of 600 Oe at the sample position. The experimental chambers were designed so that the XMCD measurement could be made immediately after film preparation without sample transfer or loss of ultrahigh-vacuum environment.

The Cu(001) single crystal was cleaned by ion bombardment and annealing. The fcc Co(001) and fcc Ni(001) thin-film substrates were grown on the clean Cu(001) crystal at room temperature by evaporation from pure Co and Ni wires. Fe films of different thickness were deposited at room temperature, by evaporation from a pure Fe wire. The base pressure of the vacuum chamber was 2×10^{-10} Torr, and the pressure during evaporation was below 2×10^{-9} Torr. LEED was used to determine substrate and film order. The film thickness was monitored by a quartz crystal microbalance located at the sample position. The calibration of the microbalance was checked using two methods. First, photoemission intensities of substrate and overlayer were measured and corrected to absolute intensities using atomic cross sections. Second, a similar procedure was applied to the substrate and overlayer x-ray absorption intensity. The agreement between the three independent film thickness measurements indicates that our reported film thickness values are accurate to within 20%. This accuracy has also been confirmed by comparing our magnetization vs film thickness measurements for Fe, Co, and Ni films grown on Cu(001) to previously published results.

Two geometries were used for the XMCD measurements, as shown in Fig. 1. To measure perpendicular magnetization, the sample normal was aligned parallel to the applied magnetic field and the photon angle of incidence on the sample was 45° [Fig. 1(a)]. To measure magnetization parallel to the

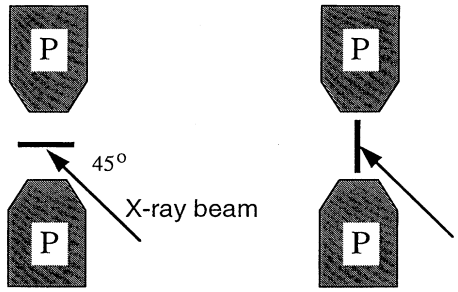

a) M perpendicular b) M parallel

FIG. 1. Experimental geometry for (a) magnetization perpendicular to the sample surface and (b) parallel to the sample surface. The sample S is rotated 90° to change the measurement geometry. The electromagnet P produces a maximum field of 600 Oe at the sample position. Circularly polarized photons from the synchrotron are incident at a 45° angle for both geometries.

surface, the sample normal was aligned perpendicular to the magnetic field and the photon angle of incidence on the sample was again 45° [Fig. 1(b)]. XMCD spectra were taken at room temperature by switching the direction of the magnetic field and measuring the total electron yield, $Y(\hbar\omega)$, while sweeping the incident photon energy at a fixed polarization. Element-specific magnetometry measurements were made by varying the magnetic field while measuring the yield at a photon energy fixed at the L_3 maximum. We report the as-acquired values of the dichroism intensities, which should be corrected for the incomplete polarization and nonparallel alignment of magnetization and photon spin for comparison to theory or other magnetization measurements. High-voltage grids were located near the sample in order to extract the electrons for the total yield measurement.

There are a number of important reasons why the specific measurement geometry of Fig. 1 was chosen. We have shown earlier[21] that the approximation $\sigma(\hbar\omega)\propto\hbar\omega Y(\hbar\omega)$ is not always valid for studies of magnetic films with photon angles of incidence greater than 50°. This is due to saturation effects in the total electron yield. Our geometry was chosen so that the approximation $\sigma(\hbar\omega)\propto\hbar\omega Y(\hbar\omega)$ is valid to within 5%.[21] The symmetry of our experimental geometry allows a direct comparison of the XMCD intensities between the parallel and perpendicular magnetization cases. We can use XMCD magnetic hysteresis loops as a function of the applied field direction to unambiguously determine the easy axis of magnetization.

III. MAGNETIC PHASES OF Fe

The magnetic properties of Fe thin films grown on fcc Cu(001), Co(001), and Ni(001) were investigated by XMCD over a thickness range from 1 to 20 monolayers (ML). As an example of the dichroism spectra used for analysis, in Fig. 2 we show the Fe and Co σ_+, σ_-, and σ_M spectra for a 4 ML film of Fe grown on the fcc Co substrate. These spectra were obtained with in-plane magnetization. Also shown in Fig. 2 are the Fe and Co XMCD hysteresis curves for both in-plane (parallel) and perpendicular magnetization. For Fe films of

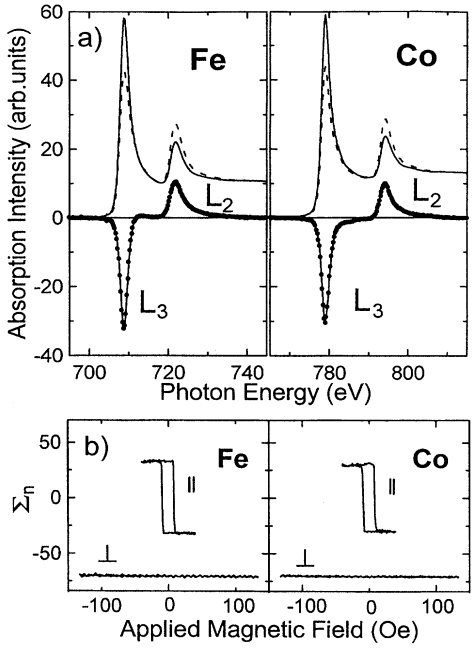

FIG. 2. (a) Fe and Co σ_+ and σ_- spectra for a 4 ML Fe/10 ML Co/Cu(001) sample (top) and their difference, $\sigma_M=\sigma_+-\sigma_-$ (bottom), showing ferromagnetic ordering in both the Fe and Co films. The spectra were taken with the sample magnetized in plane along the ⟨110⟩ direction. (b) Element-specific hysteresis curves of the same sample for magnetization parallel, ||, and perpendicular, ⊥, to the sample surface. The hysteresis curves were obtained by setting the photon energy at the L_3 peak maximum. The identical shapes of the Fe and Co hysteresis curves show that the Fe film and Co film are ferromagnetically coupled.

this thickness on Co(001), ferromagnetic ordering is detected for in-plane magnetization, but not for magnetization perpendicular to the sample surface. The Co and Fe hysteresis loops for in-plane magnetization have identical coercive fields and similar shapes, showing that the Fe and Co are ferromagnetically coupled. The XMCD spectra and XMCD hysteresis loops shown in Fig. 2 are unsmoothed data typical of the results from our experiments, which benefit from the long-term stability of the polarization and intensity at the 10 M TGM beam line.

The normalized Fe dichroism intensities at L_3 measured at remanence, Σ_R(Fe), were found to vary greatly depending on Fe film thickness and substrate. Figure 3 shows a graph of Σ_R(Fe) as a function of Fe film thickness on the three substrates we studied. For Fe growth on Cu(001), no ferromagnetic ordering is observed for films less than 10 ML thick. Above 10 ML the films are ferromagnetically ordered in plane as shown by the nonzero dichroism intensity. The saturation in Σ_R(Fe) at 14 ML shows that the entire film is magnetized at this thickness.

Three regions of different magnetic behavior are found for Fe growth on the ferromagnetic substrates fcc Co(001) and fcc Ni(001). These regions are characterized by different values of Σ_R(Fe). For coverages less than 4 ML, the Fe is ferromagnetically aligned as determined by the large value of Σ_R(Fe)~32%. This is the largest value of Σ_R(Fe) we have measured to date. For bcc Fe/Cu(001) we find Σ_R(Fe)=26%,

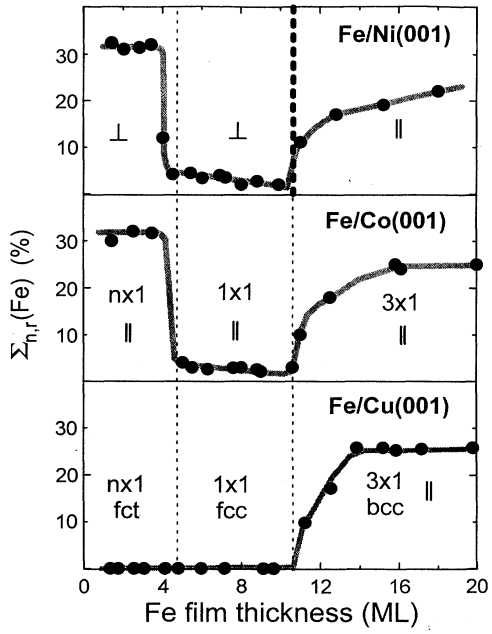

FIG. 3. Normalized dichroism intensities of Fe measured at remanence, Σ_R(Fe), which is proportional to the average vector magnetic moment per Fe atom, vs film thickness for growth on Cu(001), Co(001), and Ni(001). The vertical dashed lines represent regions of different growth for Fe/Cu(001), fct, fcc, and bcc. Different surface reconstructions, as observed by LEED, are given for Fe growth on Cu(001) and Co(001). The symbols ⊥ and ∥ signify magnetic alignment perpendicular and parallel to the sample surface, respectively. The ⟨110⟩ direction was used for the in-plane magnetic measurements. The heavy dashed line at 11 ML, for growth on Ni(001), highlights a transition in the direction of ferromagnetic alignment.

and for bcc Fe films grown on Ir(111), Σ_R(Fe)=27%.[22] The large value of Σ_R(Fe) may be due to an enhanced moment in the ultrathin Fe films. However, it is also possible that complex domain structures, due to the growth modes of bcc Fe on Cu(001) and Ir(111), may reduce the value of Σ_R(Fe) for Fe grown on these other substrates, so that the 32% figure should be considered the limiting value for Fe. The easy axis of magnetization is in plane along ⟨110⟩ for 1–4 ML of Fe on Co(001). At the same thickness on Ni(100), the easy axis is perpendicular to the surface.

Between 5 and 11 ML, Σ_R(Fe) is reduced to nearly zero for growth on both Co and Ni, in a transition which occurs over a very narrow thickness range. The easy axis of magnetization for this thickness range remains in plane for growth on Co, ⟨110⟩, and perpendicular to the surface for growth on Ni. For coverages greater than 11 ML, Σ_R(Fe) increases. For growth on Co, Σ_R(Fe) at 16 ML coverage is nearly equal to Σ_R(Fe) for thick bcc Fe films grown on Cu(001). For growth on Ni, Σ_R(Fe) gradually increases over the thickness range from 12 to 18 ML, but does not quite reach the value of Σ_R(Fe) for thick bcc Fe films grown on Cu(001). The easy axis of magnetization for Fe films thicker than 11 ML switches from perpendicular to the surface to in plane for Fe films grown on Ni and remains in plane for Fe films grown on Co(001).

It is important to examine the magnetization of the substrate before discussing the results presented in Fig. 3. In Fig.

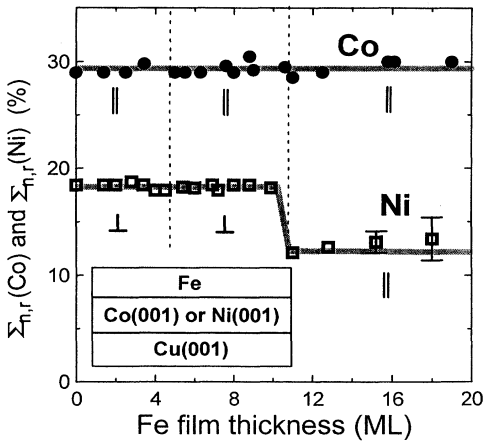

FIG. 4. Normalized dichroism intensities of the Co and Ni substrates vs Fe coverage. The error bars for Σ_R(Ni) for thicker Fe films are due to the weak Ni absorption cross section and the increased background signal due to the Fe overlayers.

4 we show the values of Σ_R(Co) and Σ_R(Ni) vs Fe coverage. Σ_R(Co) does not change with Fe coverage and the easy axis of magnetization is always in the surface plane. For Fe/Ni, Σ_R(Ni) is 18% for Fe coverages less than 11 ML and 12% for Fe coverages greater than 11 ML. This change in Σ_R(Ni) is accompanied by a change in the easy axis of magnetization which is perpendicular to the surface for coverages below 11 ML and in plane for coverages above 11 ML. The decrease in Σ_R(Ni) may be due to complex magnetic domain structures in the Ni films magnetized in plane.

An important advantage of the XMCD technique is that we independently measure the magnetization of the ferromagnetic overlayer (Fe) and substrates (Ni or Co), which is what is displayed in Figs. 3 and 4. The sharp decline in the Fe magnetization near 5 ML has no counterpart in the substrate signals. The rise in Fe magnetization above 11 ML is absent in the Co data, and for Ni there is an opposite behavior at this point. This means that the magnetization changes seen in the Fe films at 5 and 11 ML must be due to phase changes in the Fe itself, rather than arising from changes in the substrate magnetization.

These large changes in the magnetic properties of the Fe films grown on Co and Ni are accompanied by structural changes in the Fe films between 5 and 11 ML coverage. The dashed lines in Fig. 3, at 5 and 11 ML, separate the regions of different crystal structures found for Fe growth on Cu(001).[1,2] The onset of ferromagnetic ordering at 11 ML for Fe/Cu(001) is due to the antiferromagnetic fcc to ferromagnetic bcc phase transition. We do not see magnetic ordering in the fcc phase (5–11 ML), since we are measuring at room temperature. Both the Néel temperature of the fcc phase (T_N=200 K) and the Curie temperature of the live surface bilayer (T_c=250 K) are below room temperature.[2] Similarly, we observe no perpendicular magnetization for fct Fe/Cu(001) films (5 ML and below), since room temperature is only slightly below the Curie temperature of these films.

The regions of different magnetic behavior of Fe for growth on Co and Ni nearly coincide with the regions of different crystal structure for Fe growth on Cu. This is strong evidence that Fe has the same growth mode on Cu(001),

Co(001), and Ni(001). Further evidence comes from LEED. For Fe growth on Co, we observe $(n\times1)$, $n=4$ or 5, diffraction patterns for Fe coverages less than 5 ML, (1×1) diffraction patterns for Fe coverages between 5 and 11 ML, and (3×1) diffraction patterns for coverages greater than 11 ML. This is identical to the LEED results we obtain for Fe growth on Cu(001) and is in agreement with published LEED results for Fe/Cu(001).[2] For Fe growth on Ni(001), we do not observe sharp higher-order diffraction spots, just intensity modulated streaks along the $\langle 110\rangle$ directions. Given the identical surface unit cells of the three substrates, the coincidence of the changes in magnetism with anticipated changes in crystalline structure, and the identical surface reconstructions for growth on Cu(001) and Co(001), we propose that the sequence of structures for Fe grown on Ni(001) and Co(001) is the same as for Fe growth on Cu(001).

The magnetic transitions of the Fe/Co and Fe/Ni thin films (Fig. 3) can now be explained in terms of the structural changes in the films and the influence of the magnetic substrates. At coverages below 5 ML the Fe films grow in the fct structure, which is ferromagnetic.[2] Ferromagnetic ordering is evident in the large dichroism intensity we find for films between 1 and ~4 ML thick. The Curie temperature of ultrathin ferromagnetic films is dependent on film thickness, and for many thin film systems $T_C=0$ K at 1 ML thickness.[15] This is the reason we do not observe ferromagnetic ordering for fct Fe/Cu(001) at room temperature. In contrast, the exchange coupling between the (Co, Ni) substrates and the Fe overlayers results in ferromagnetic ordering for fct Fe/Co(001) and Fe/Ni(001) films down to <1 ML thickness at room temperature.

Between 5 and 11 ML the Fe films grow with a fcc structure. For growth on Cu(001), fcc Fe is an antiferromagnet with a Néel temperature below room temperature ($T_N=200$ K). Since the Néel temperatures for the Fe/Cu(001), Fe/Co(001), and Fe/Ni(001) films are likely to be similar, at room temperature these films will be nonmagnetic, which gives zero dichroism intensity. However, the dichroism signal in this phase is greatly reduced, but does not go to zero. This nonzero dichroism intensity is due to magnetism at the Fe/Co and Fe/Ni interfaces, which we discuss in detail in the next section. Above 11 ML, the critical thickness for fcc Fe growth is exceeded, and the Fe films gradually transform into the bcc structure. This is the room-temperature stable crystal structure, and it is ferromagnetic, which is evident in the increase in the dichroism intensity.

IV. MAGNETISM AT THE INTERFACE

In this section we focus attention on the fcc phase of the Fe/Co(001) and Fe/Ni(001) films, which corresponds to the 5–11 ML thickness range. The nonzero dichroism intensity found for this phase of Fe is interesting to study in detail, for it highlights the interface effects on magnetism. These interface effects on magnetism are important for the understanding of spin-dependent scattering at the interface, which is believed to be a major factor in giant magnetoresistance.

The most likely location for the ferromagnetically ordered Fe is either at the overlayer/substrate interface or at the surface of the overlayer. No ferromagnetic ordering is found for fcc Fe/Cu(001) at room temperature, and so by comparison it

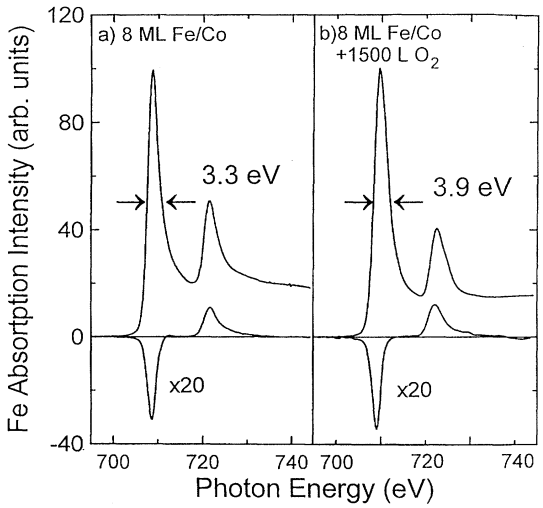

FIG. 5. Fe $L_{2,3}$ absorption spectra $\sigma_+ + \sigma_-$ and normalized dichroism spectra σ_M for (a) an 8 ML film of fcc Fe/Co(001) and (b) the same film after exposure to 1500 L of O_2. The width of the Fe L_3 peak is increased after oxygen exposure due to the formation of Fe oxides at the surface. The Fe L_3 dichroism peak position and width do not change upon exposure to oxygen, showing that the magnetically aligned Fe is not on the surface.

is clear that the magnetic substrate is responsible for the ordering in the fcc Fe films grown on Ni and Co. Exchange coupling is short range, which suggests that the magnetically aligned Fe is at the interface. However, fcc Fe films on Cu(001) are known to have a ferromagnetically live surface bilayer.[1,2] The Curie temperature of such a bilayer for growth on Co(001) or Ni(001) should be comparable to that for Fe on Cu ($T_C=250$ K), so that for room-temperature measurements we must consider the possibility of ferromagnetic surface layers.

To determine if the magnetically live layer is at the Fe-vacuum or Fe-substrate interface, we have made XMCD measurements on fcc Fe/Co samples before and after exposure to O_2. In Fig. 5 we show the absorption spectra $(\sigma_+ + \sigma_-)$ and the dichroism spectra σ_M for an 8 ML fcc Fe/Co(001) film before and after exposure to 1500 L of O_2. Following this exposure the Fe L_3 absorption peak is broadened from 3.3 to 3.9 eV. This is due to the formation of Fe oxides, whose L_3 absorption peaks are shifted to higher photon energy. Comparison of peak areas shows that 3 ML of Fe have been oxidized. Nevertheless, the absolute intensity, position, and width of the L_3 *dichroism* peak is not altered by exposure to oxygen. The relative intensity of the L_3 dichroism peak does increase upon exposure to O_2, but this is an artifact due to the broadening of the L_3 absorption spectra. The ferromagnetically aligned Fe is not altered by the surface oxidation. We conclude that the ferromagnetically live Fe in the fcc Fe/Co films is located at the Fe/Co interface. The overall similarity of the Fe/Co and Fe/Ni systems implies that the ferromagnetic live layer lies at the Fe/Ni interface in that system as well, though we did not explicitly repeat the oxidation experiment in this case.

Dichroism intensities can be used to determine how much Fe is magnetically aligned at the interface. By measuring the

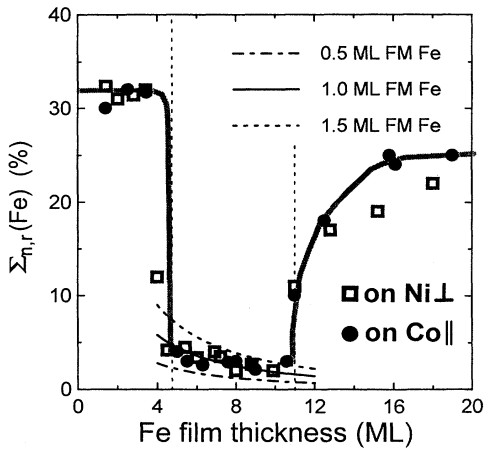

FIG. 6. Magnetism of fcc Fe films grown on fcc Co(001) and fcc Ni(001) compared to calculations assuming 0.5, 1.0, and 1.5 ML of ferromagnetic Fe at the Co/Fe interface. The vertical dashed lines are from Fig. 3 and the thick gray line is included as a visual aid only.

dichroism intensity of a sample with known magnetic properties, the dichroism intensity Σ_R can be quantified. If it is assumed that the local magnetic moment of an individual atom is the same in the two samples then the fraction of atoms magnetically aligned in the unknown sample can be determined from changes in Σ_R. This type of transferability argument works only when comparing dichroism spectra of the same element.

Before determining the amount of magnetically aligned Fe in the fcc phase, we discuss possible uncertainties in this type of analysis. Changes in the L_3 absorption line shape due to changes in crystalline structure may affect the value of Σ_R independent of changes in magnetic moment. Our experience is that changes in the Fe L_3 line shapes for Fe in different metallic environments are very small. This is in contrast to the large changes we have measured for the Mn L_3 line shape.[12,22,23] This suggests that Σ_R(Fe) is a good measure of the Fe moment for Fe in different metallic environments, but that Σ_R(Mn) will not be a good measure of the Mn moment for Mn in different metallic environments. Changes in the ground state expectation values of $\langle L_z \rangle$ and $\langle S_z \rangle$ affect the intensity of the L_3 dichroism peak through the dichroism sum rules.[24] To test the magnitude of this uncertainty we have compared the XMCD line shapes for fct and bcc Fe and find them to be nearly identical, showing that the uncertainty due to changes in $\langle L_z \rangle$ and $\langle S_z \rangle$ is negligible for this experiment. Of course, changes in resolution, degree of circular polarization, alignment of sample magnetization with photon spin vector, and presence of multiple magnetic domains all affect the value of Σ_R. It is therefore important to make these comparisons using the same experimental conditions and to ensure that the measurements are made along the easy axis of magnetization on samples with square hysteresis loops.

With these cautions in mind, XMCD intensities for fcc Fe/Co(001) and fcc Fe/Ni(001) have been used to determine how much Fe is magnetically aligned at the fcc Fe/Co and fcc Fe/Ni interfaces. In Fig. 6 the element-specific magnetization is plotted for the Fe in both the Fe/Co and Fe/Ni films. All films in the fcc Fe thickness region have square hysteresis loops and show ferromagnetic coupling between the magnetically live Fe and substrate. The Σ_R(Fe) values for $\perp$ fcc Fe/Ni(001) are similar to values for $\parallel$ fcc Fe/Co(001). The predicted dichroism intensities assuming 0.5, 1.0, and 1.5 ML of ferromagnetically aligned Fe at the interface are compared to the experimental results in Fig. 6. For this analysis we used an exponential dependence of the electron yield with film thickness, using an effective probing depth of 20 Å verified through experiment on calibrated wedge samples.[13] A normalized dichroism intensity of Σ_R(Fe)=26% was used as the value expected for a ferromagnetic Fe film at saturation. This value was chosen from the XMCD measurements on bcc Fe films grown on Cu(001) (see Fig. 3). The model calculation in Fig. 6 shows that 1.0 ± 0.5 ML of Fe are magnetically aligned at both the Fe/Ni and Fe/Co interfaces.

The largest uncertainty in this determination of the width of the magnetically live Fe layer comes from the assumption that the magnetic moment of Fe at the interface is the same as the moment of bulk Fe. The Fe moment at the interface could be different from bulk Fe for a number of reasons, which include structural effects, alloying, or magnetic coupling. The influence on our model due to the uncertainty in the Fe moment can be estimated using results of polarized neutron studies on $Fe_xCo_{(1-x)}$ and $Fe_xNi_{(1-x)}$ alloys.[25] These studies found that the Fe moment is enhanced in both alloys, with a maximum measured moment of $\sim 3.0\mu_B$ for both the FeCo and FeNi alloys compared to $2.2\mu_B$ for bulk Fe. Setting the Fe moment in the magnetically aligned Fe layer to $3.0\mu_B$, we would reinterpret the measured XMCD intensities as corresponding to 0.75 ± 0.5 ML of magnetically aligned Fe at the Fe/Co and Fe/Ni interface rather than 1.0 ± 0.5 ML. For the present analysis we have assumed that $\Sigma_n \propto M_{\mathrm{Fe}}$, where M_{Fe} is the Fe moment, ignoring the orbital contribution to the total moment. This is justified due to solid-state quenching of the orbital moment. The thickness of the live layer derived in both approximations, 0.75 ± 0.5 and 1.0 ± 0.5 ML, is consistent with a single layer of magnetically ordered Fe, polarized by the ferromagnetic substrate.

To explore the origin of the magnetically live Fe monolayer at the Fe/Co and Fe/Ni interfaces in greater detail, we performed element-specific x-ray dichroism magnetometry measurements. In Fig. 7 we show the Ni hysteresis of a 15 ML Ni/Cu(001) film. The loop is square with a coercive field of H_C=77 Oe. In Figs. 7(b)–7(d) we show the Ni and Fe hysteresis loops for three different coverages of Fe on top of the Ni(001) film. For each coverage the H_C of the Fe and Ni hysteresis loops is identical, and the shapes are similar, showing ferromagnetic coupling. Addition of a 2.6 ML film of Fe reduces the coercive field to 34 Oe and the hysteresis loops are no longer square. The remanent XMCD, Σ_R(Fe), is reduced by $\approx 10\%$ from its saturated value. At this thickness, the Fe is in the fct phase and it is ferromagnetic with a moment perpendicular to the sample surface. For a 5.2 ML film [Fig. 7(c)], H_C increases to 65 Oe and the dichroism intensity of the Fe film decreases. This Fe is in the fcc phase, which is nonmagnetic at room temperature. The Fe dichroism intensity is greatly decreased and the moment remains perpendicular to the sample surface. For an 18 ML Fe film [Fig. 7(d)], H_C is 56 Oe. This is the ferromagnetic bcc phase of Fe and the easy axis of magnetization now lies within the surface plane.

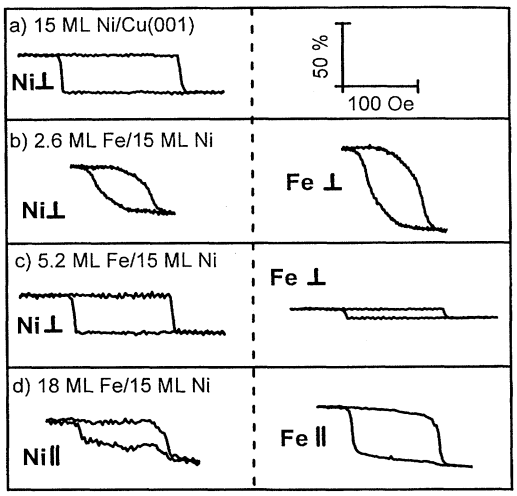

FIG. 7. Element-specific magnetometry curves of (a) a 15 ML Ni/Cu(001) film, (b) a 2.6 ML Fe/15 ML Ni/Cu(001) bilayer, (c) a 5.2 ML Fe/15 ML Ni/Cu(001) bilayer, and (d) an 18 ML Fe/15 ML Ni/Cu(001) bilayer. The height of the hysteresis loops is given as $\Sigma_n = |\sigma_M(L_3)/\sigma_0(L_3)|$, which is proportional to the average vector magnetic moment per atom.

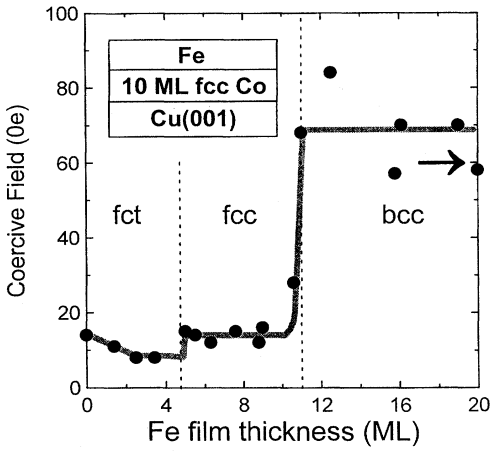

FIG. 8. Coercive field of Fe/10 ML fcc Co/Cu(001) films vs Fe coverage. The coercive field is different for the three different phases of Fe present, fct, fcc, and bcc. The arrow identifies the coercive field for a 20 ML bcc Fe/Cu(001) film.

The changes in the hysteresis loops for the Fe/Ni(001) system are somewhat unusual. The area of the Ni hysteresis loop is reduced by a factor of 2.0 after the addition of 2.6 ML of Fe. This means that the 2.6 ML Fe capping layer reduces the amount of work required to flip the spins of 15 ML of Ni. One explanation for this is that the magnetic reorientation in the Fe film is less hindered than in the Ni films. This could be due to differences in spin fluctuations or anisotropy energies in the Fe and Ni films. Larger spin fluctuations in the Fe layers could account for both the reduction in the coercive field (from 77 to 34 Oe) and the change from a square loop to one with a reduction in remanent field.

The Ni hysteresis curve for the sample covered with 5.2 ML of fcc Fe is square with $H_C = 65$ Oe. This loop returns to the original shape of the uncovered Ni film, with a small reduction in the coercive field (from 77 to 65 Oe). This is also consistent with a spin-fluctuation model for the Fe layer, if we take into account that only the interface Fe layer is ferromagnetically coupled.

The perpendicular magnetization of the Fe/Ni film is also interesting. The Ni/Cu(100) film has a transformation from parallel magnetization in the first few layers to perpendicular at higher thicknesses (above 9 ML), a behavior which is counter to what is expected from the shape anisotropy.[14–16] The surface anisotropy energy of Ni favors in-plane alignment, and it has been proposed[16] that the perpendicular orientation is due to a bulk uniaxial anisotropy in the Ni film, which is tetragonally distorted on the Cu(100) substrate, forcing the magnetization out of the surface plane. The addition of Fe layers initially favors this perpendicular anisotropy, since fcc Fe surfaces have a surface anisotropy energy of opposite sign to that of Ni.

When the Fe film thickness is increased to 11 ML, the fcc Fe structure begins to relax back to the stable bcc lattice. At this point, the easy axis of magnetization flips back into the surface plane, as it is for bcc Fe films on Cu(100). The change in remanent magnetization at the fcc-to-bcc transition is gradual, unlike the sharp fct-to-fcc transition. The gradual change to the bcc magnetization limit is probably due to a gradual transformation of the fcc structure to bcc above the critical layer thickness for supporting fcc epitaxy. However, the easy axis flips from perpendicular to parallel in a very narrow thickness range near 11 ML. The 18 ML bcc Fe/Ni(001) hysteresis loops are similar in shape to what we find for bcc Fe/Cu(001) films.

Our element-specific magnetometry results for the Fe/Ni(001) system, summarized in Fig. 7, show that the interfacial Fe layer is ferromagnetically polarized by the substrate. A similar result was found in the Fe/Co system. There are, however, some significant differences in the details of the magnetic coupling between the two bilayer systems. For the Fe/Co(001) case, unlike Fe/Ni(001), the element-specific hysteresis loops were square for both elements at all Fe coverages. In addition, at all Fe coverages studied the easy axis was in plane. Therefore we can summarize the magnetometry results by plotting the change in coercive field as a function of coverage, which is shown in Fig. 8. Each Fe film was ferromagnetically coupled to the Co substrate as determined by the similar shapes of the Co and Fe hysteresis curves. The coercive field for an uncapped Co film is 15 Oe. This is reduced to 8 Oe when capped by the addition of fct Fe. When the Fe thickness is increased into the fcc, antiferromagnetic range, the coercive field is restored to the uncapped value, in the same manner as was found for the Fe/Ni system. In the bcc phase, the coercive field rises to the value found for bcc Fe/Cu(001), shown by the arrow in Fig. 8.

Magnetically coupling fct Fe to fcc Co decreases H_C by almost a factor of 2, while coupling bcc Fe to fcc Co increases H_C by almost a factor of 5. These changes in the coercivity can be interpreted in the same way as the sequence of changes found in the Fe/Ni system, although the absolute magnitude of the coercivity in the various thickness ranges are different. Spin fluctuations in the ferromagnetic, fct Fe layers reduce H_C, up to the structural transition to the fcc phase. At this point, only the interface Fe layer is ferromag-

netically coupled, and the coercivity rises to the value for the uncapped Co film. At thicker Fe coverages, the film changes over to bcc, and the coercivity for the Fe/Co bilayer is determined by the Fe.

The magnetic alignment of the Fe atoms at the fcc Fe/Ni and fcc Fe/Co interfaces is induced by the ferromagnetic substrate. At room temperature, the fcc Fe capping layer becomes an unusual magnetic structure, in which ferromagnetically aligned Fe interface atoms are in contact with magnetically disordered Fe layers, though all of the Fe atoms have large local moments. Because of induced ferromagnetic ordering at the interface, the magnetic interface is not identical to the compositional interface. The Fe/Co and Fe/Ni interfaces are undoubtedly not atomically sharp, and Fe is soluble in both Ni and Co, so that some intermixing is expected, though the extent of this awaits future detailed structural measurements. The magnetic/nonmagnetic interface is located, on average, 1 ML beyond the nominal Fe/Co or Fe/Ni interface. This is true, independent of any intermixing of the two elements. The difference in position of the magnetic and compositional interfaces should be taken into account in any studies of spin scattering in Fe/Co or Fe/Ni multilayers.

V. SUMMARY AND CONCLUSIONS

We have investigated the magnetic phases of ultrathin films of Fe grown on fcc Co(001) and fcc Ni(001). The two substrates, 10 ML fcc Co/Cu(001) and 15 ML fcc Ni/Cu(001), are both ferromagnetic with the direction of magnetization in the surface plane for Co and perpendicular to the surface plane for Ni. A sequence of three distinct magnetic phases of Fe is found for growth on both Ni and Co. An identical sequence of magnetic phase transitions is known to occur for Fe growth on Cu(001). For Fe growth on Cu(001), these magnetic phase transitions are caused by crystalline phase transitions due to the growth mode of Fe on Cu(001). Based on these comparisons and on the nearly identical lateral lattice constants of fcc Co(001), Ni(001), and Cu(001), we conclude that Fe growth on fcc Co(001) and Ni(001) follows the same sequence of crystalline phase transitions as Fe growth on Cu(001). These results are supported by LEED, which shows an identical sequence of surface reconstructions for Fe growth on fcc Co(001) and Cu(001). For Fe growth on Ni(001), the surface reconstructions are not well defined, suggesting that the details in the growth mode of Fe on Ni(001) are different.

Fe films less than 5 ML thick crystallize in the fct structure and are ferromagnetic. The Curie temperature of these fct Fe films is increased by the presence of the ferromagnetic substrates, allowing ferromagnetic ordering to be observed down to ~1 ML coverage at room temperature. These Fe films have a larger dichroism intensity than any other Fe films we have studied. This may be due to an enhanced surface or interface moment. The moments of the fct Fe films are aligned perpendicular to the surface for growth on Ni(001) and in the surface plane for growth on Co(001).

A transition from ferromagnetic Fe to a nonmagnetic phase occurs in a very narrow thickness range beginning near 5 ML. Fe films between 5 and 11 ML thick crystallize in the fcc structure and are nonmagnetic at room temperature. These nonmagnetic fcc Fe films contain a monolayer of ferromagnetically aligned Fe at the Fe/Co and Fe/Ni interface. The magnetic alignment of Fe in these films is induced by the ferromagnetic substrates, effectively extending the magnetic/nonmagnetic interface. The moments of the magnetically live Fe monolayer are aligned perpendicular to the surface for growth on Ni(001) and in the surface plane for growth on Co(001). Fe films thicker than 11 ML transform to the bcc structure and are ferromagnetically ordered. The moments of the bcc Fe films are aligned in the surface plane for growth on both Co(001) and Ni(001).

Coupled ferromagnetic bilayers are a natural extension of the study of ultrathin magnetic films and sandwich structures with a single ferromagnetic component. The properties of these films, as we have found for Fe/Ni and Fe/Co, are not the same as for growth on nonmagnetic substrates and are not simply related to the magnetic properties of the corresponding alloys, which makes them interesting. With an element-specific magnetic probe, such as x-ray dichroism, it is possible to separately determine the polarization in each of the ferromagnetic components, making it possible to see such subtle effects as the magnetically live Fe interface layer.

There is sufficient novelty in the Fe/Co(001) and Fe/Ni(001) systems to justify the additional work necessary to clarify the magnetic phase diagram. Interface and surface anisotropy energies need to be measured for these bilayer systems in order to understand the observed changes in magnetization direction. Element-specific magnetometry measurements need to be made at lower temperatures, to remove ambiguities arising from the change in Curie temperature with film thickness. Similarly, the Curie temperatures of the two coupled layers should be determined. Finally, additional structural studies are needed to understand the growth modes and verify our proposed assignment of crystalline structures.

ACKNOWLEDGMENTS

This work was supported by the National Science Foundation, Division of Materials Research under Grant No. DMR-94-13475. The Synchrotron Radiation Center is a national facility supported by the NSF Division of Materials Research.

[1] J. Thomassen, F. May, B. Feldmann, M. Wuttig, and H. Ibach, Phys. Rev. Lett. **69**, 3831 (1992).

[2] D. Li, M. Freitag, J. Pearson, Z. Q. Qiu, and S. D. Bader, Phys. Rev. Lett. **72**, 3112 (1994).

[3] P. Xhonneux and E. Courtens, Phys. Rev. B **46**, 556 (1992).

[4] H. Magnan, D. Chandesris, B. Villette, O. Heckmann, and J. Lecante, Phys. Rev. Lett. **67**, 859 (1991).

[5] F. J. Himpsel, Phys. Rev. Lett. **67**, 2363 (1991).

[6] D. P. Pappas, K.-P. Kämper, and H. Hopster, Phys. Rev. Lett. **64**, 3179 (1990).

[7] J. G. Tobin, G. D. Waddill, and D. P. Pappas, Phys. Rev. Lett. **68**, 1943 (1992).

[8] K. Kalki, D. D. Chambliss, K. E. Jonson, R. J. Wilson, and S. Chiang, Phys. Rev. B **48**, 18 344 (1993).
[9] H. Li and B. P. Tonner, Surf. Sci. **237**, 141 (1990).
[10] M. T. Kief and W. F. Egelhoff, Phys. Rev. B **47**, 10 785 (1993); D. A. Steigerwald and W. F. Egelhoff, Jr., Surf. Sci. **192**, L887 (1987).
[11] D. Weller, G. R. Harp, R. F. C. Farrow, A. Cebollada, and J. Sticht, Phys. Rev. Lett. **72**, 2097 (1994).
[12] J. Zhang, Z.-L. Han, S. Varma, and B. P. Tonner, Surf. Sci. **298**, 351 (1993).
[13] W. L. O'Brien and B. P. Tonner, Phys. Rev. B **50**, 2963 (1994).
[14] W. L. O'Brien and B. P. Tonner, Phys. Rev. B **49**, 15 370 (1994).
[15] F. Huang, M. T. Kief, F. J. Mankey, and R. F. Willis, Phys. Rev. B **49**, 3962 (1994).
[16] B. Schulz and K. Baberschke, Phys. Rev. B **50**, 13 467 (1994).
[17] M. G. Samant, J. Stöhr, S. S. P. Parkin, G. A. Held, B. D. Hermsmeier, F. Herman, M. van Schilfgaarde, L. C.-Duda, D. C. Mancini, N. Wassdahl, and R. Nakajima, Phys. Rev. Lett. **72**, 1112 (1994).
[18] Y. U. Idzerda, L. H. Tjeng, H. J. Lin, C. J. Gutierrez, G. Meigs, and C. T. Chen, Phys. Rev. B **48**, 4144 (1993).
[19] C. T. Chen, Y. U. Idzerda, H.-J. Lin, G. Meigs, A. Chaiken, G. A. Prinz, and G. H. Ho, Phys. Rev. B **48**, 642 (1993).
[20] R. W. C. Hansen, W. L. O'Brien, and B. P. Tonner, Nucl. Instrum. Methods Phys. Res. A **347**, 148 (1994).
[21] W. L. O'Brien and B. P. Tonner, Phys. Rev. B **50**, 12 672 (1994).
[22] W. L. O'Brien and B. P. Tonner, Vac. Sci. Technol. A **13**, 1544 (1995).
[23] W. L. O'Brien and B. P. Tonner, Phys. Rev. B **51**, 617 (1995).
[24] P. Carra, B. T. Thole, M. Altarelli, and X. Wang, Phys. Rev. Lett. **70**, 694 (1993).
[25] M. F. Collins and J. B. Forsyth, Philos. Mag. **8**, 401 (1963).